Regular Article

PHYSICAL CHEMISTRY RESEARCH
Published by the
Iranian Chemical Society
www.physchemres.org
info@physchemres.org

***Phys. Chem. Res.**, Vol. 5, No. 3, 447-463, September 2017*
DOI: 10.22036/pcr.2017.72765.1351

Hydrogen Adsorption on (5,0) and (3,3) Na-decorated BNNTs

H.A. Shafiei Gol and M. Noura
Physics department, Science Faculty, University of Sistan and Baluchestan, Zahedan, Iran.
(Received 23 January 2017, Accepted 2 March 2017)

The storage capacity of hydrogen on Na-decorated born nitride nanotubes (BNNTs) is investigated by using density functional theory within Quantum Espresso and Gaussian 09. The results obtained predict that a single Na atom tends to occupy above the central region of the hexagonal rings in (5,0) and (3,3) BNNT structures with a binding energy of -2.67 and -4.28 eV/Na-atom, respectively. The single H_2 molecule that is absorbed by a Na decorated BNNTs changes the electrostatic field around Na atom, and consequently changes the charge of the participating atoms in the interaction region. According to Mulliken population and partial density of state (PDOS) analyses, positive charge carried by Na atoms decreases. Another result of this charge transfer reveals an increase in the magnitude of the dipole moment of BNNT-Na-1H_2 with respect to BNNT-Na. The results of charge density, separation distance of atoms in adsorption region as well as the H_2 binding energy show the hydrogen molecule adsorption is a physical adsorption (physisorption). In the adsorption process, a single sodium atom with losing about 0.4e of its net charge can adsorb up to six H_2 molecules with the binding energy of -0.35 and -0.32 eV/H_2 molecule on (5,0) and (3,3) BNNTs, respectively. Comparing the H_2 binding energies of two nanotubes implies that (5,0) BNNT-Na is more desirable for the hydrogen molecule adsorption than (3,3) BNNT.

Keywords: Density functional theory, BNNT, Partial charge density, Charge transfer, Dipole moment, Hydrogen storage

INTRODUCTION

Discovery of carbon-based nanomaterials such as fullerene, graphene and carbon nanotubes has opened a new window in materials science and technology due to their light weight and large surface to volume ratio for hydrogen storage. However, these nanomaterials cannot be of much benefit for hydrogen adsorption due to weak van der Waals interactions between hydrogen molecules and the surface atoms of the carbon nanomaterials to retain H_2 in room temperature. Therefore, this problem has attracted the attention of scientists and researchers to corporation of metals (alkali [1-3], alkaline [4-8] and transition metals [9-17]) on carbon nanomaterials. Lee *et al.* investigated hydrogen adsorption and storage in carbon nanotubes (CNTs) experimentally and theoretically. They reported that hydrogen exists to form H_2 molecule in an empty space inside CNTs which was confirmed by their Raman spectra. Also, their theoretical calculations predicted that hydrogen storage capacity on (10,10) nanotubes could exceed 14% (160 kg H_2/m^3) [18]. Yildrim and Ciraci carried out a first-principle study, demonstrating that a single Ti atom with four hydrogen molecules can coat on a single-walled nanotube (SWNT). At high Ti coverage, a SWCNT can strongly adsorb hydrogen up to 8% [19]. According to the studies of Y. Ye and *et al.* hydrogen adsorption on SWCNT was found to exceed 8%, which is the highest capacity of any carbon material. They reported that at pressures higher than about 40 bar at 80 K, a phase transition occurs where there is a separation of the individual SWCNTs, and hydrogen is physisorbed on their exposed surface [20]. Liu *et al.* synthesized masses of SWCNTs with a large mean diameter of about 1.85 nm in order to adsorb hydrogen. They achieved a hydrogen storage capacity of 4.2 weight percent or hydrogen to carbon atom ratio of 0.52 at room temperature under a modestly high pressure (about 10

*Corresponding author. E-mail: shafiei@phys.usb.ac.ir

megapascal) for a SWCNT sample of about 500 m weight. They suggest that SWCNT can be an effective hydrogen storage material because the SWCNT can be easily produced and it shows reproducible and modestly high hydrogen uptake at room temperature [21].

Although, from structural point of view, boron nitride (BN) materials are similar to carbon materials such as nanotubes, the calculation carried out by Oku and Narita based on first-principle method predicts that BN fullerene materials and their stability for high temperature are expected to be good [22]. Dillon *et al*. reported that open-end carbon nanotubes can store H_2 gas by using capillary action up to 5-10 wt% ; however, when carbon nanotubes are doped by alkali metals, they can store H_2 gas under ambient pressure and moderate temperature up to 20 wt% [23]. Shahzad Khan and his colleague e investigated hydrogen adsorption on potassium-decorated boron nitride nanotubes. They found that the hydrogen adsorption on (3,3) and (5,0) K-decorated BNNTs is about 8.5 wt% and 9.4 wt%, respectively. Single-wall carbon nanotubes (SWCNT), depending on their diameter and helicities, can show semiconducting or metallic behaviour, while BNNTs are semiconductors with a wide band gap whose band gap is independent of tube diameter and helicities [24].

BNNTs are more stable thermally and chemically as well [25-27], therefore, they can be good candidates for hydrogen storage. In this paper, we investigate hydrogen molecule storage on (3,3) and (5,0) Na-decorated boron nitride nanotubes (BNNTs). Details of computational works based on density functional theory (DFT) and its corresponding approximations are presented in section 2. In section 3, first the physical properties of (5,0) and (3,3) BNNTs decorated with 1H2-Na up to 8H2-Na, and then BNNTs with more Na atoms up to 5 and 6 are studied. Finally, the last section presents the results of our study.

COMPUTATIONAL DETAIL

All calculations have been performed using Born-Oppenheimer approximation [28], within the framework of DFT [29]. Also, Kohn-Sham formalism [30] as self-consistency has been used to solve the single particle equations of electronic structures with quantum ESPRESSO package [31]. In DFT calculations, we have used the local density approximation (LDA) in Ceperley and Alder (CA) form, as approximated by Perdew-Zunger (PZ) for exchange and correlation function. Moreover, relativistic effects are employed for atoms participating in nanotubes within calculations. In this method, which is called the scalar relativistic approximation (SRA), the spin-orbit coupling term appearing in Dirac's equations is dropped. Occasionally, the minority component of the wave function is also neglected in defining the charge density [32]. Configurations of $2s^2 2p^1$ of B, $22s^2 2p^3$ of N, $3s^1$ of Na and $1s^1$ of H atoms are treated as valence in pseudo potential description, respectively.

After optimizing and imposing periodic conditions on supercell sizes for each nanotube, dimensions of simulated supercells ranged from $28 \times 28 \times 37$ Å^3 for the smallest systems to $46 \times 46 \times 37$ Å^3 for the largest systems, respectively. The wave functions were expanded in a plane wave basis set with the kinetic energy cutoff 70 Ry. Calculations were also performed at the center of the Brillouin zone (Γ-point only). Initial geometries of nanotubes placed at the Γ-point were optimized by using conjugate gradient (CG) method [33] with a convergence value 1×10^{-4} eV in total energy of nanostructure. Also, a convergence criterion 0.09 eV/Å was imposed for each force component.

RESULTS AND DISCUSSION

Hydrogen Adsorption on a Single Na Atom-decorated BNNT

Initially, the (3,3) and (5,0) boron nitride nanotubes decorated with a single sodium atom were investigated to understand the hydrogen adsorption phenomena. In order to remove the effect of dangling bonds at the end of the nanotubes, 10 and 12 hydrogen atoms were added to the (5,0) and (3,3) BNNTs, respectively. The result obtained based on our studies [34] shows that the hexagonal center of B_3N_3 on the BNNT surface is the most favorable position to adsorb a single Na atom. It is also observed that two atoms of the mentioned hexagonal ring are closer to Na dopant compared to four other atoms. The binding energy of a decorated Na atom on (3,3) BNNT determined using the following formula:

$$E_B(Na) = \left\{ \frac{E_{TOT}(BNNT) + E_{TOT}(mNa) - E_{TOT}(BNNT - mNa)}{m} \right\}$$

shows that the adsorption strength of a single Na atom on (3,3) BNNT is about 1.59 eV/Na-atom more than (5,0) BNNT (-2.69 eV/Na-atom) due to differences in the curvature of their surfaces [35]. Here, E_{TOT} is the total energy of corresponding optimized structure and 'm' is the number of the adsorbed Na atoms.

In such conditions, a single H_2 molecule is placed near Na atom, and then the system under review is relaxed. Initial separation of H_2 and Na is chosen based on their chemical considerations such as H-Na and H-H bonds. These optimized structures are shown in Figs. 1a, b.

The results obtained from the optimized structure show that when the H_2 molecule is adsorbed, the average nearest-neighbor distance of Na atom from tubular surface changes from 2.96 Å to 2.80 Å for (5,0) BNNT and 2.78 Å to 2.79 for (3,3) BNNT and the H_2 molecule tends to be at a distance of about 2.53 Å and 2.49 Å from Na atom in (5,0) and (3,3) BNNT-1Na structures, respectively. Moreover, the H-H bond is increased from 0.70 Å in the molecular state to 0.771 Å and 0.768 Å for (5,0) and (3,3) BNNT-1Na, respectively, which can be attributed to the interaction between H atoms and Na atom.

The highest effect of the adsorbed hydrogen molecule is revealed on the electronic properties of the Na decoration BNNTs. The H_2 molecule interacts with Na atom with the binding energy of -0.35 eV/H_2 and -0.41 eV/H_2 for (5,0) and (3,3) BNNT-1Na, respectively, which indicates more stability of H_2 molecule on (3,3) BNNT-1Na. This energy has been calculated by:

$$E_B(H_2) = \left\{ (E_{tot}(host) + E_{tot}(nH_2) - E_{tot}(host - nH_2))/n \right\}$$

where, E_{tot} is the total energy of corresponding optimized structure and 'n' represents the total number of adsorbed H_2 molecules. These small adsorption energies of hydrogen molecules on BNNTs can be attributed to van der Waals interaction of H-H and H-Na exhibiting a physical adsorption (or physisorption) characteristic which can easily be broken even at low temperature. This feature is very beneficial for the release of hydrogen in the desired locations. Also, the H_2 molecule adsorption decreases the band gap energy of (5,0) BNNT-1Na about 0.01 eV and increases that about 0.16 eV for (3,3) BNNT-1Na.

The change in the separation distance of Na atom from the surface atoms of BNNT-1Na (after doping H_2 molecule) implies a charge transfer between dopant atoms and the BNNT-1Na structure. This arises from a difference in their electronegativity which creates a dipole moment for the corresponding structure. According to Mulliken charge calculations obtained based on DFT as well as B3LYP [36] within Gaussian09 package [37], it is observed that the ionization of Na atom in the adsorption process of the H_2 molecule on BNNT-1Na has been enhanced so that the positive charge carried by Na atom decreases from 0.87e to 0.84e on (5,0) BNNT and from 0.85*e* to 0.83*e* on (3,3) BNNT. In the hexagonal ring near Na atom, H_2 dopant leads to decrease the total charge of B atoms in the range of (1.157, 1.152) *e* and increase the charge of N atoms in the range of (-1.502, -1.504)*e* on (5,0) BNNT-1Na-H_2. This charge transfer takes place in the range of (1.061, 1.115) *e* and (-1.516, -1.520) *e* for B and N atoms in (3, 3) BNNT-1Na-H_2, respectively. Moreover, the results show that H_2 adsorption (due to the charge transfer) decreases the magnitude of the dipole moment vector of (5, 0) BNNT-1Na from 15.98 D (1D = 3.33564×10^{-30} C m) to 15.04D and increases the magnitude of the dipole moment vector of (3,3) BNNT-1Na from 10.32 D to 11.78 D. In the adsorption process of the H_2 molecule, the charge of hydrogen atoms undergoes major changes and is localized around atoms with asymmetrical distribution of 0.008 *e* and 0.007 *e* on (3,3) and 0.0009 *e* and 0.006 *e* on (5,0)BNNT-1Na-H_2's. The H_2 molecule is polarized with the positive charge of Na atom. There is no charge transfer between H_2 and Na atom.

As seen in Fig. 1, hydrogen molecule in BNNT-1Na-1H_2 structure has lain at the top of Na atom, and its H-H axis is approximately parallel to the nanotube axis. Therefore, the electron cloud distributed around H-H atoms (Figs. 2a, b), which arises from overlapping *s* atomic orbitals, seems to be symmetrical and parallel to that of BNNT. This overlap leads to a covalent type of binding known as σ binding. Nevertheless, there is no overlap between the electron cloud of H and Na atoms in the H2-Na region. This feature can confirm the physical adsorption of hydrogen on BNNT-1Na. In addition, the Na atom causes to

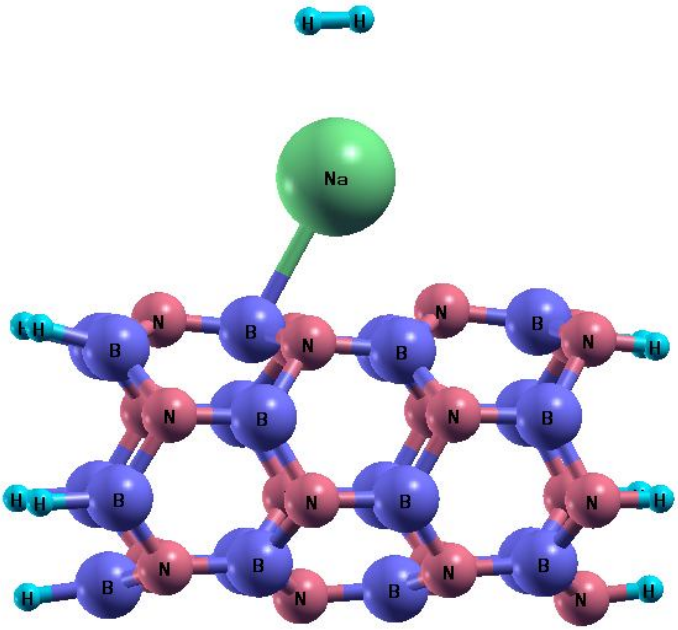

(a)

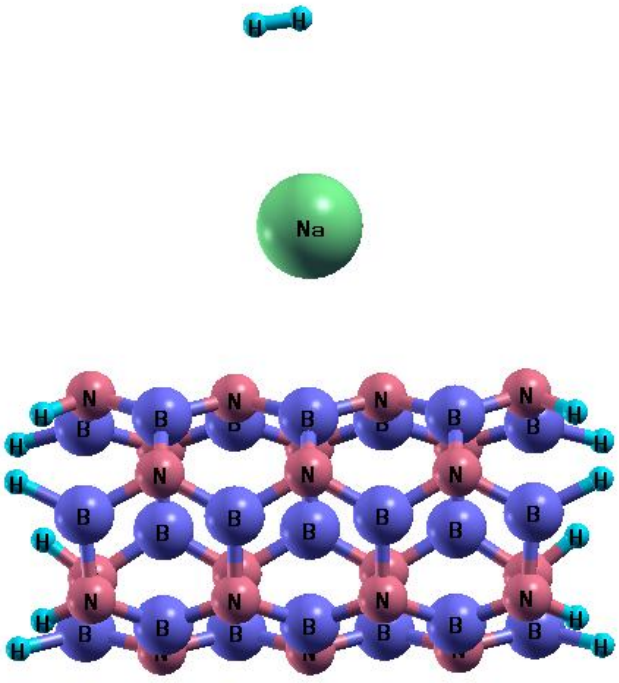

(b)

Fig. 1. Optimized geometries of (a) (5,0) and (b) (3,3) BNNT-1Na structures with one H_2 molecule.

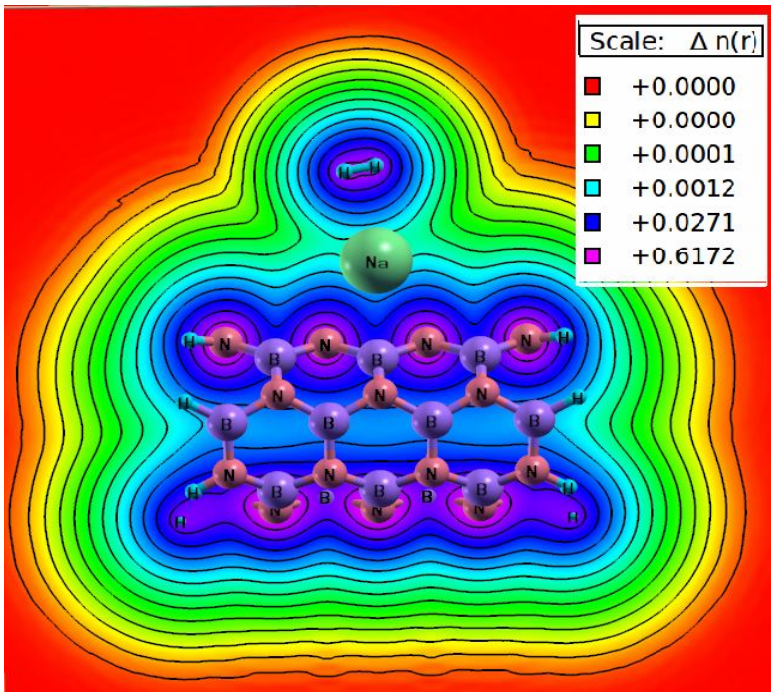

(a)

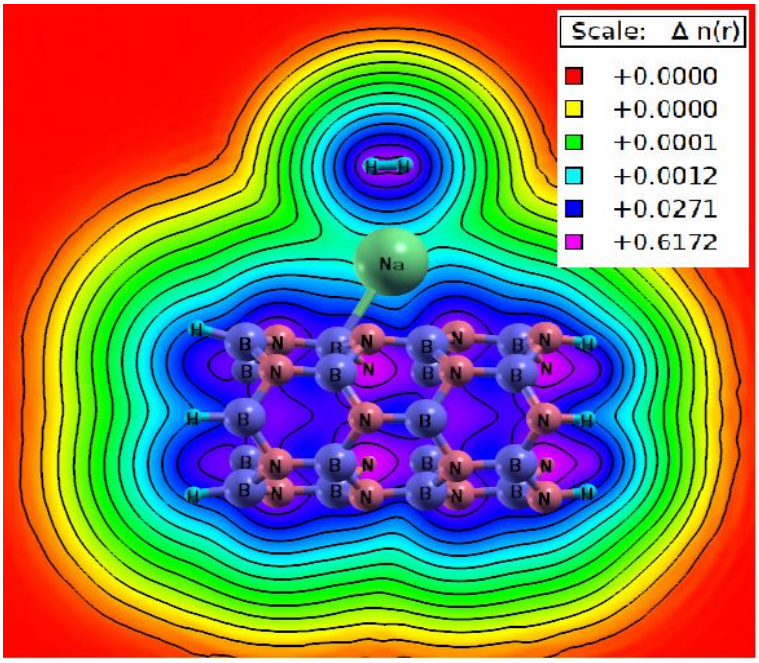

(b)

Fig. 2. Charge density contour plot of H_2 on (a). (5,0) and (b) (3,3) BNNT-1Na.

change the symmetry of the contour lines so that the electron charge distribution is distorted toward BNNT structure. In the inside nanotube region, the charge density with large value in contour scale has been localized in a wide area around N atoms with respect to B atoms. These features reveal a covalent type of binding though with a large ionicity.

Adsorption of Multiple H_2 Molecules

In this step, the BNNT-1Na structures under study are allowed to be relaxed with two H_2 molecules (**Fig. 3**). The results of the optimized geometries show that there is no change in the separation of H_2 molecules and Na atom in (5,0) BNNT as compared to (5,0) BNNT-1Na decorated with a single H_2 molecule (BNNT-1Na-1H_2), while the separation of H_2 molecules and Na atom increases about 0.037 Å with respect to (3,3) BNNT-Na-1H_2. The adsorption of the second H_2 molecule resulted in an increase in binding energy in values 0.29 eV for (5,0) and a decrease in values 0.45 eV for (3,3) with respect to (5,0) and (3,3) BNNT-Na-1H_2. Also, the second H_2 molecule disturbs the charge distribution in the interaction region and causes to reveal a strong electric field around the Na atom due to the charge transfer. Amongst, Na atom carries a 0.831e charge, whereas H atoms carry charges of 0.017*e* and -0.002*e* on (5,0) BNNT. Similarly for (3,3) BNNT, the 0.814*e* charge is localized on Na and 0.001*e* and 0.005*e* on H atoms.

Figures 3 and 4 show the optimized geometries of the (5,0) and (3,3) BNNT-Na covered with H_2 molecules up to 8. The results related to these structures, including average adsorption distance, average H_2 bond length, charge localized on Na, and binding energy per H_2 are summarized in Tables 1 and 2. As seen in Table 1, a single Na atom can adsorb H_2 molecules up to eight. The results show that as the number of H_2 molecules increases, the initial H_2 molecules adsorbed on Na atom leave their previous positions and after interaction with the added H_2 molecule reach to a new symmetric configuration. In other words, there is a slow increase in the adsorption distance as the number of H_2 molecules increase. This is because of the weak binding of the H_2 molecules to a single Na atom and their coulomb repulsion with each other. These data may suggest that the most appropriate number of H_2 molecules which can be adsorbed to a single Na atom is about 6 molecules.

The Mullikan population analysis shows that the charges localized on Na atom and its surrounding atoms are redistributed due to their interactions. So, the distributed charge around the Na atom (based on data given in Tables 1 and 2) follows a decreasing trend with increasing the number of the H_2 molecules. In this case, the Na atom appears as the positively charged atom which loses part of its charge to BNNT, and on the other hand, adsorbs H_2 molecules with coulomb interactions. As seen in Tables 1 and 2, the magnitudes of the H_2 adsorption energies are less than 1 eV for both (5,0) and (3,3) BNNT-Na implying the physisorption of hydrogen on BNNTs-Na. Also, these results can be deduced from Figs. 3 and 4 in which hydrogen atoms have retained the molecular structure. This range of the adsorption energy comes in good agreement with the previously reported average binding energy of hydrogen, 0.09 to 0.22 eV for one to eight molecules, in the potassium-adsorbed (5,0) and (3,3) BNNTs system [24]. A comparison of the H_2 binding energy of two nanotubes implies that the H_2 adsorption energy on (5,0) is less than that of (3,3) BNNT-1Na. Therefore, the (5,0) BNNT-1Na is more favorable for H_2 adsorption.

energy is inversely proportional to the average distance between the adsorbed H_2 and Na atom as the number of H_2 molecules increases. This can be attributed to the increase of coulomb repulsion among H_2 molecules as well as H_2 molecules with Na atom.

Uniform Na-decoration (5,0) and (3,3) BNNT

Now, we investigate the adsorption ability of the mentioned BNNTs with more Na atoms. The output of the calculations obtained for the (5,0) and (3,3) BNNTs decorated with three Na atoms (Figs. 5a, b) shows that the average distance between sodium atoms and the B_3N_3 hexagons is 2.61 Å and 2.74 Å for (5,0) and (3,3) BNNTs which has decreased about 0.21 Å and 0.05 Å with respect to those of BNNTs-1Na. Also, the separation distance of sodium atoms from each other are 7.51, 4.35, 7.61 Å in (5,0) BNNT-3Na and 7.27, 7.35,7.17 Å in (3,3) BNNT-3Na which are much larger than the Na-Na distance, 3.12 Å, in Na bulk [44]. This separation may be considered as an important factor in the adsorption of Na atoms on BN

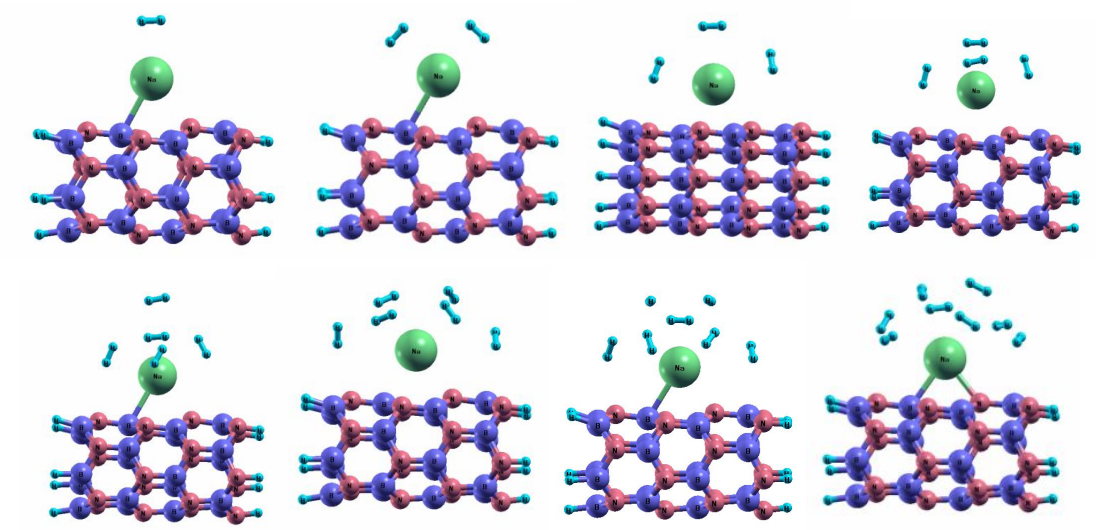

Fig. 3. Adsorption of one to eight H_2 molecules on (5,0) BNNT-1N.

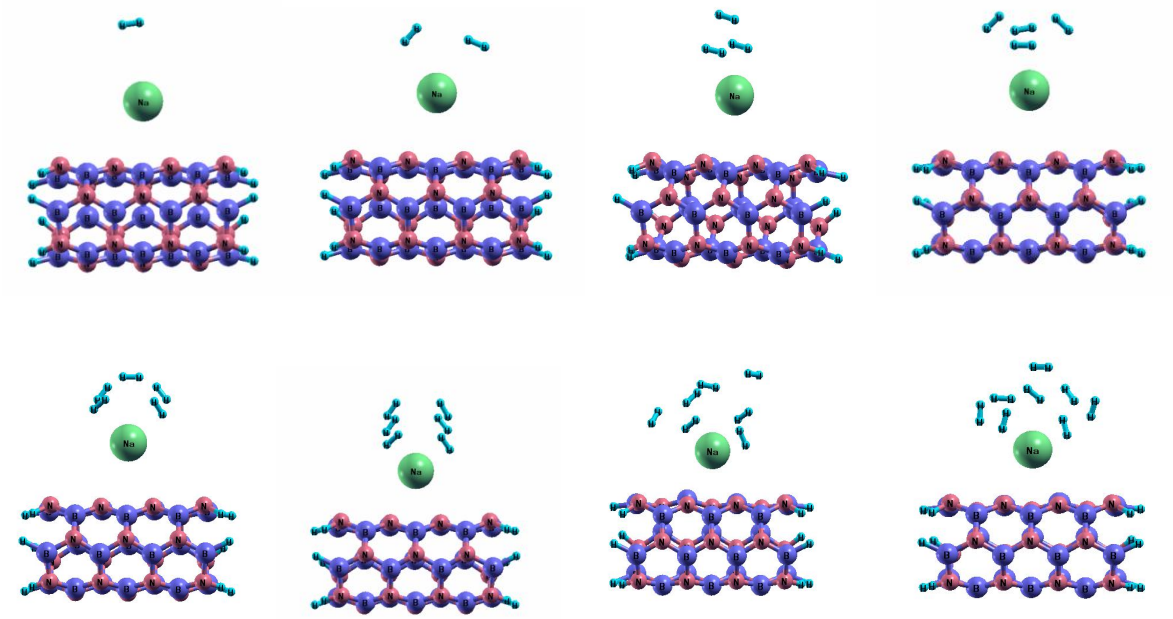

Fig. 4. Adsorption of one to eight H_2 molecules on (3,3) BNNT-1Na.

nanotubes. From the energetic point of view, sodium atoms retain their positions on B_3N_3 hexagons of nanotubes with a binding energy of -1.49 eV/Na and -1.53 eV/Na for (5,0) and (3,3), respectively, which are -0.36 and -0.39 eV lower than that of its Bulk [44]. This feature implies that sodium atoms can come in the form of clusters on BNNT surface. Moreover, as the number of sodium atoms increases, the more charge transfer occurs between Na atoms and nanotube, so that the charge per Na atom is decreased to the values of 0.78, 0.39, 0.30*e* on (5,0) and 0.84, 0.83, 0.84 *e* on (3,3) BNNTs-3Na and consequently, the magnitude of the dipole moment changes from 6.28D to 14.83D for (5,0) and

Table 1. The Bond length, Charges on Na and Binding Energy of Na (eV/Na) and H_2 (eV/H_2) on (5,0) Na-BNNT

System	Average adsorption distance	Average H_2bond length (Å)	Charge on Na(e)	Binding energy (eV)
$0H_2$	2.92	-	0.869	-2.69 (without H_2)
$1H_2$	2.53	0.7718	0.842	-0.4080
$2H_2$	2.48	0.7714	0.831	-0.4488
$3H_2$	2.54	0.7746	0.838	-0.4488
$4H_2$	2.53	0.7741	0.821	-0.4325
$5H_2$	2.72	0.7732	0.814	-0.3672
$6H_2$	2.98	0.7707	0.832	-0.3536
$7H_2$	3.06	0.7731	0.831	-0.2274
$8H_2$	3.16	0.7768	0.808	-0.1928

Table 2. The Bond Length, Charges on Na and Binding Energy of Na (eV/Na) and H_2 (eV/H_2) on (3,3) Na-BNNT

System	Average adsorption distance	Average H_2 bond length (Å)	Charge on Na	Binding energy (eV)
$0H_2$	2.78	-	0.850	-4.1839 (without H_2)
$1H_2$	2.49	0.7689	0.832	-0.3125
$2H_2$	2.85	0.7690	0.814	-0.2895
$3H_2$	2.95	0.7697	0.826	-0.3738
$4H_2$	2.86	0.7693	0.826	-0.4024
$5H_2$	2.60	0.7725	0.805	-0.3960
$6H_2$	2.63	0.7710	0.808	-0.3196
$7H_2$	3.08	0.7711	0.807	-0.4043
$8H_2$	3.09	0.7714	0.800	-0.4595

om 0.12D to 1.13D for (3,3) BNNT-3Na with respect to their pure BNNTs. It is also seen that doping of three Na atoms reduces the band gap of (5, 0) BNNT from 2.25 eV to 0.32 eV and from 4.26 eV to 0.31 eV for (3,3).

Then, to get a configuration with uniform coverage, the (5,0) and (3,3) BNNTs are decorated by five and six Na atoms, respectively (Figs. 6a, b). This number of sodium atoms are directly related to the number of the hexagonal rings covering the BNNT surface. In this case, the average distance of sodium atoms from the hexagons reaches to a

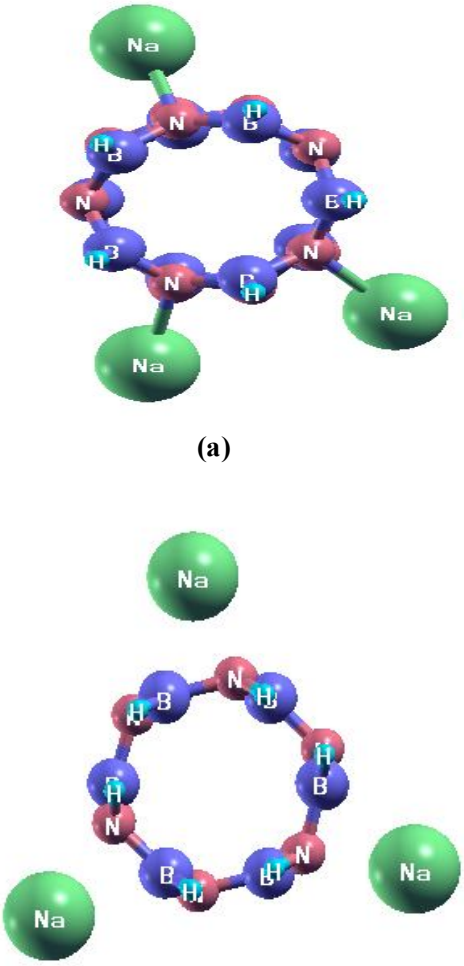

(a)

(b)

Fig. 5. Optimized structure of (a) (5,0) and (3,3) BNNT-3Na.

value of 2.61 Å and 2.80 Å for (5,0) BNNT-5Na and (3,3) BNNT-6Na, respectively. The distance of sodium atoms from each other is equal to 4.59, 4.91, 4.55, 4.09, 4.08 Å in (5,0) BNNT-5Na and 4.40, 4.38, 4.42, 4.41, 4.76, 4.63 Å in (3,3) BNNT-6Na which are larger than the Na-Na distance in Na bulk, 3.12 Å [44].

These relative ely charge is just due to the electrostatic repulsion between Na atoms which can be considered as an adsorption region for each Na atom.

It is predicted that Na atoms are revealed in a clustering form in BNNT structures with high Na atoms, since the binding energy per Na atom for (5,0) and (3,3) BNNTs is lower (-1.02 eV and -0.96 eV, respectively) than the cohesive energy of (-1.13 eV) bulk Na [44]. Indeed, the clustering decreases the reaction energy of H_2 [45]. Ipso facto, the charge per Na atom decreases to a value of 0.227, 0.189, 0.228, 0.259, 0.300e for (5,0) BNNT-5Na and 0.691, 0.684, 0.631, 0.481, 0.478, 0.546e and (3,3) BNNT-6Na, respectively.

The partial density of state (PDOS) of BNNTs before/after high Na decoration is shown in Figs. 7a, b. As seen in both figures, the unoccupied orbitals above the Fermi level (which are observed in the PDOS of the pure BNNTs) cut Fermi level and shift toward lower energies. This can be attributed to the charge transfer between the Na atoms and the BNNT structure which creates metallic

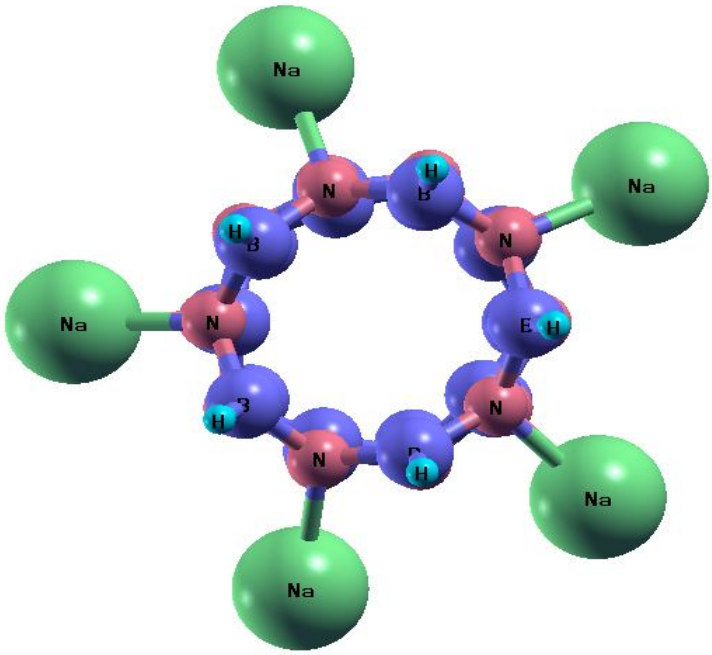

(a)

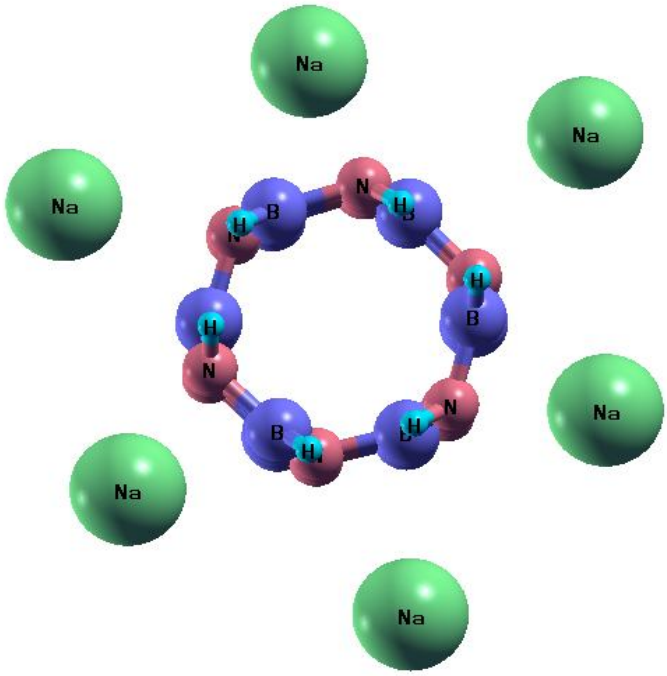

(b)

Fig. 6. Optimized structure of (a) (5,0) BNNT-5Na (b) (3,3) BNNT-6Na.

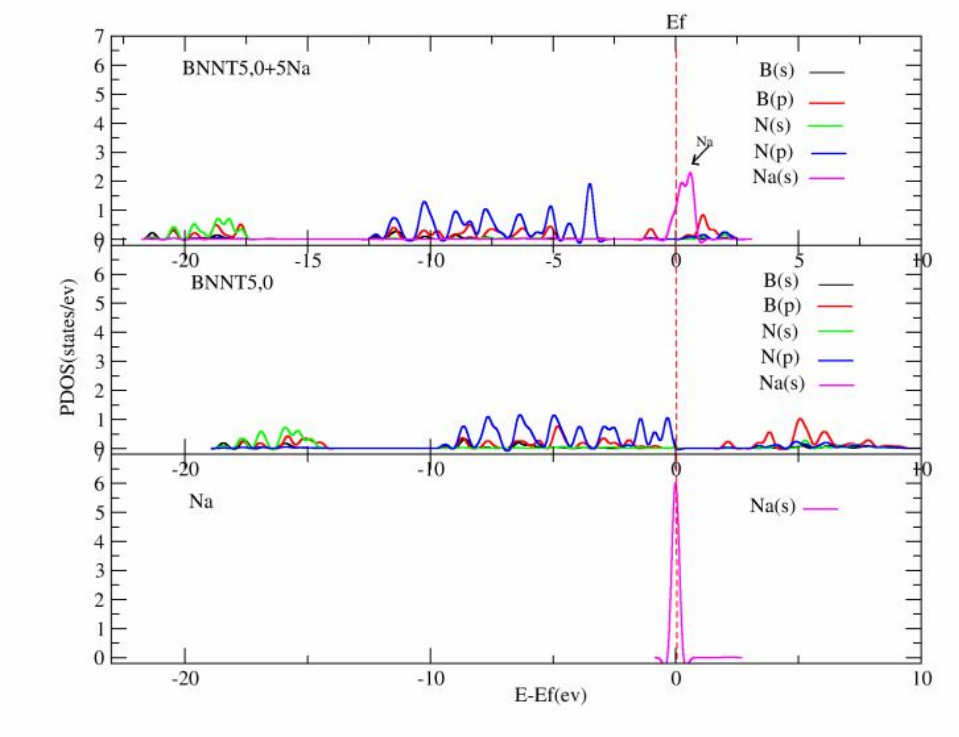

(a)

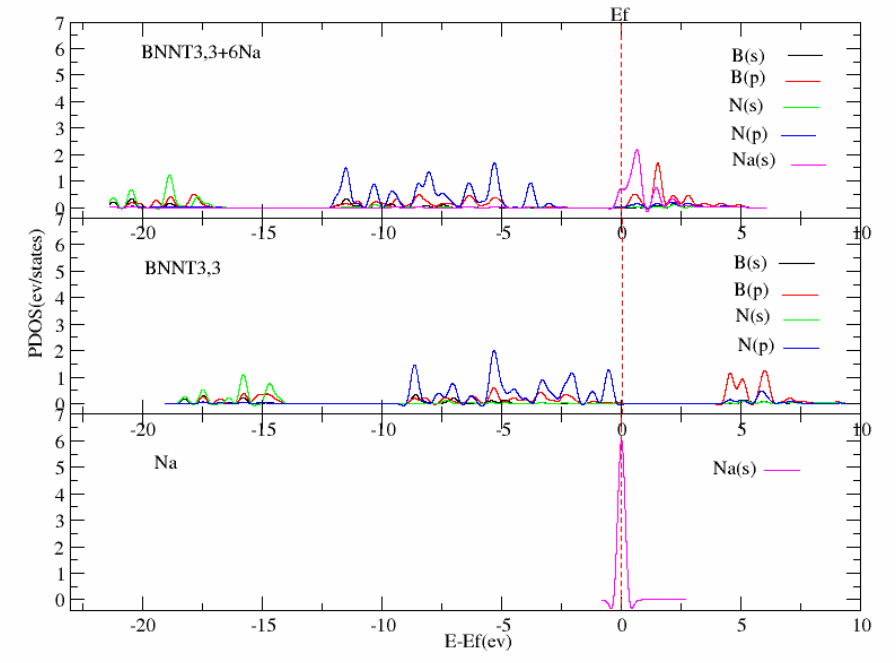

(b)

Fig. 7. PDOS of (a). (5,0) BNNT-5Na (b) (3,3) BNNT-6Na.

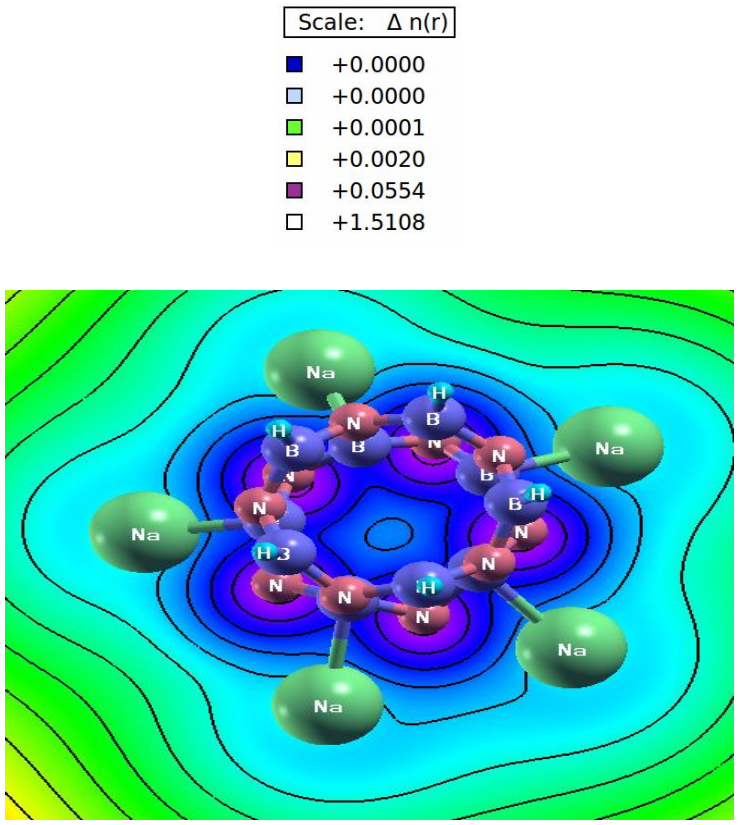

(a)

(b)

Fig. 8. Charge density contour plots of (a) BNNT-5Na and (b) (3,3) BNNT-6Na from the front view.

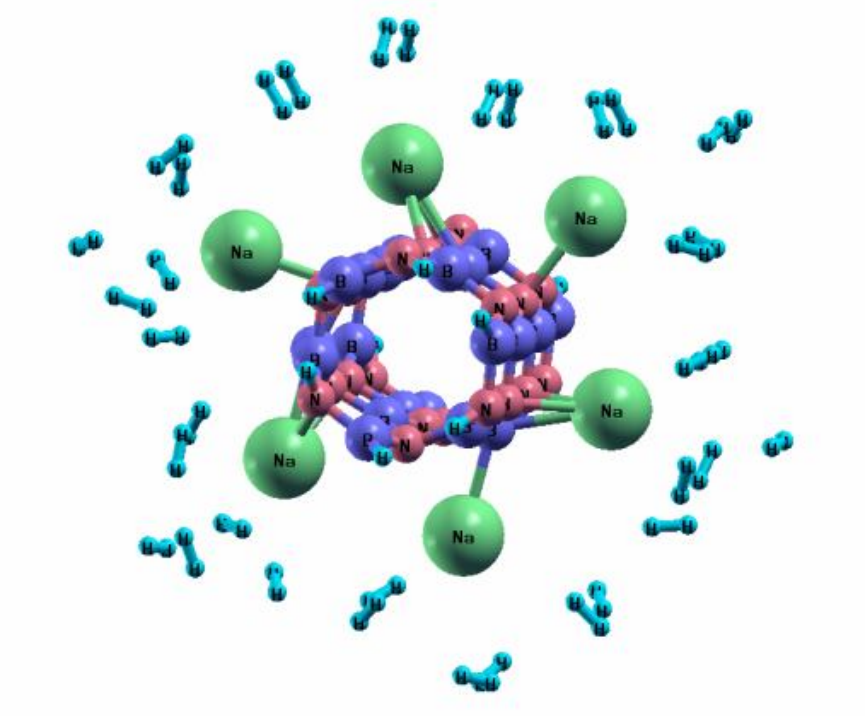

(a)

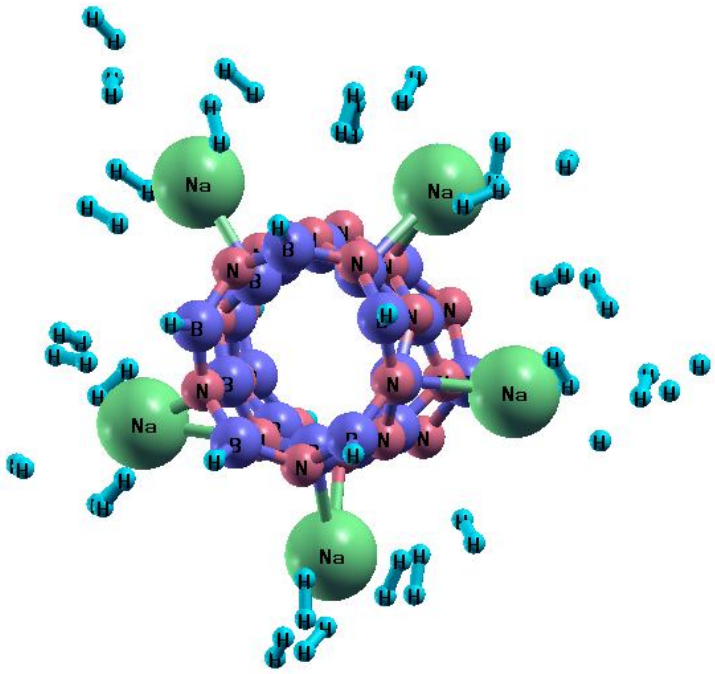

(b)

Fig. 9. Optimized configurations of (a) (5,0) BNNT-5Na-30H_2 and (b) (3,3) BNNT-6Na-36 H_2.

character for BNNTs decorated with high Na atoms. Also, in both figures there is a decrease in the peak of Na occupied s orbital after decorated which is related to the charge transfer between Na and the nanotubes.

Mulliken population analysis shows that the average amount of charge on sodium atoms due to the charge transfer to surrounding (5,0) BNNT-5Na and (3,3) BNNTs-6Na reduces to 0.25*e* and 0.47*e*, respectively. From the above discussion, it is clear that the charge transfer can change the magnitude of the dipole moment, from 6.2816 D for pure (5,0) to 8.92 for (5,0) BNNT-5Na and from 0.12D for pure (3,3) BNNT to 1.47D for (3,3) BNNT-6Na.

In the last step, the total charge density contour plots are presented for the 5 and 6 Na-decorated systems in Figs. 8a, b from the front view.

As seen in both figures, clustering of Na atoms is observable with their bonding to nanotube (in Fig. 8a) or changing the contour lines around Na atoms (in Fig. 8b) which is different from those of the preceding nanotubes. The contour lines are distributed symmetrically around Na atoms and nanotube. Such symmetry is also observed around B and N atoms, however due to the high electronegativity of N atom with respect to B atom, the charge contribution localized (based on its large value in contour scale) around N atoms is more than that of B atoms. For these reasons, the interaction between atoms in BNNT reveals a covalent type of binding though with a large ionicity.

Hydrogen Adsorption in (5,0) and (3,3) BNNT with Uniform Na Decoration

The (5,0) BNNT with the uniform Na decoration can adsorb at most thirty H_2 molecules with binding energy of -0.37 eV/H_2, whereas this number is increased to thirty-six H_2 molecules with binding energy of -0.44 eV/H_2 for (3,3) BNNT. The results obtained based on the optimized geometries, shown in Figs. 9a, b, imply that hydrogen atoms still maintain their configurations in molecular forms in both nanotubes. In the present systems, (5,0) and (3,3) BNNTs with uniform Na-decoration have a maximum gravimetric storage capacity of 8.87 wt% and 9.75 wt%, respectively, for high Na-decorated (5,0) and (3,0) BNNTs, respectively, which is higher than the revised 2020 target for on-board automobile applications. The US Department of Energy has set a target to achieve 5.5 wt% gravimetric density for hydrogen storage in light-duty vehicles by 2020 [46].

CONCLUSIONS

The adsorption mechanism of hydrogen molecule on (5,0) and (3,3) boron nitride nanotube decorated with Na atoms (BNNT-1Na) has been investigated by using density functional theory (DFT) under the local density approximation (LDA) in the Ceperley and Alder (CA) form. Results show that in adsorption of a single hydrogen molecule on BNNT-1Na, distance of the sodium atom from the center of the hexagonal ring and H-H distance in the hydrogen molecule undergoes changes. The origin of these changes is related to the electrostatic field around Na atom and consequently charge transfer in the interaction region in which the Na atom loses about 0.03e of its net charge in the (5,0) and 0.02e in (3,3) BNNT-Na. Moreover, in this region, the net charge of N atoms increases and the net charge of B atoms decreases. The analysis of charge density, separation distance of atoms in adsorption region, and the adsorption energy of hydrogen molecule imply that the hydrogen adsorption is a physical adsorption. The partial density of state analysis shows the adsorption of the hydrogen molecules on the BNNT structures decorated with high Na atoms revealing the metallic character for the BNNT-1Na-H_2s. The (5,0) and (3,3) BNNT structures decorated with high (5 and 6) Na atoms in a symmetrical form are able to adsorb 30 and 36 hydrogen molecules, respectively, where Na atoms seem to be in a clustering form to the BNNTs decorated with high Na atoms.

REFERENCES

[1] Liu, W.; Zhao, Y. H.; Jiang, Y.; Li, Q.; Lavernia, E. J., Enhanced hydrogen storage on Li-dispersed carbon nanotubes, *J. Phys. Chem. C* **2009**, *113*, 2028-2033, DOI: 10.1021/jp8091418.

[2] Wang, F. D.; Zhang, N. N.; Li, Y. H.,; Tang, S. W.; Sun, H.; *et al.* High-capacity hydrogen storage of Na-decorated graphene with boron substitution: first-principles calculations, *Chem. Phys. Lett.* **2013**, *555*, 212-216.

[3] Froudakis, G. E; Why alkali-metal-doped carbon

nanotubes possess high hydrogen uptake. *Nano. Lett.* **2001**, *1*, 531-533, DOI: 10.1021/nl0155983.

[4] Hussain,T.; Pathak, B.; Ramzan, M.; Mark, T. A.; Ahuja, R., Calcium doped graphene as a hydrogen storage material. *Appl. Phys. Lett.* **2012**, *100*, 183902, DOI: http://dx.doi.org/10.1063/1.4710526.

[5] G. Kim, G.; Jhi, S.; Lim, S.; Park, N., Crossover between multipole Coulomb and Kubas interactions in hydrogen adsorption on metal-graphene complexes. *Phys. Rev. B.* **2009**, *79*, 155437, DOI: 10.1103/ PhysRevB.79.155437.

[6] Cazorla, C.; Shevlin, S. A.; Guo, Z. X., First-principles study of the stability of calcium-decorated carbon nanostructures. *Phys. Rev. B.* **2010**, *82*, 155454, DOI: https://doi.org/10.1103/PhysRevB. 82.155454.

[7] Lee, H.; Huang, B.; Duan, W.; Ihm, J., *Ab initio* study of beryllium decorated fullerenes for hydrogen storage, *J. Appl. Phys.* **2010**, *107*, 084304, DOI: http://dx.doi.org/10.1063/1.3387750.

[8] Lee, H.; Ihm, J.; Cohen, M. L.; Louie, S. G., Calcium-decorated graphene-based nanostructures for hydrogen storage. *Nano. Lett.* **2010**, *10*, 793-798, DOI: 10.1021/nl902822s.

[9] Reyhani, A.; Mortazavi, S. Z.; Mirershadi, S.; Moshfegh, A. Z; Parvin, P.; Golikand, A. N., Hydrogen storage in decorated multiwalled carbon nanotubes by Ca, Co, Fe, Ni and Pd nanoparticles under ambient conditions. *J. Phys. Chem. C.* **2011**, *115*, 6994-7001, DOI: 10.1021/jp108797p.

[10] Fair, K. M.; Cui, X. Y.; Li, L.; Shieh, C. C.; Zheng, C. C.; Liu, Z. W., Hydrogen adsorption capacity of adatoms on double carbon vacancies of graphene: a trend study from first principles. *Phys. Rev. B.* **2013**, *87*, 014102, DOI: https://doi.org/10.1103/PhysRevB. 87.014102.

[11] Yildirim, T.; Ciraci, S., Titanium-decorated carbon nanotubes: a potential high-capacity hydrogen storage medium, *Phys. Rev. Lett.* **2005**, *94*, 175501, DOI: https://doi.org/10.1103/PhysRevLett.94.175501.

[12] Bhattacharya, S.; Majumder, C.; Das, G. P., Hydrogen storage in Ti decorated BC4N nanotube, *J. Phys. Chem. C.* **2008**, *112*, 17487, DOI: 10.1021/ jp807280w.

[13] Wu, M.; Gao, Y.; Zhang, Z.; Zeng, X. C., Edge-decorated graphene nanoribbons by scandium as hydrogen storage, *Nanoscale.* **2015**, *4*, 915- 920. DOI: 10.1039/c2nr11257d.

[14] Kim, G.; Jhi, S.; Lim,S.; Park, N.; Effect of vacancy defects in graphene on metal anchoring and hydrogen adsorption, *Appl. Phys. Lett.* **2009**, *94*, 173102, DOI: 10.1063/1.3126450.

[15] Lopez-Corral, I.; German, E.; Juan, A.; Volpe, M. A.; Brizuela, G. P., Hydrogen adsorption on palladium dimer decorated graphene: a bonding study, *Int. J. Hydrogen Energy.* **2012**, *37*, 6653-6655, DOI: 10.1016/j.ijhydene.2012.01.039.

[16] Liu, Y. C. M.; Brown, D. A.; Neumann, D. P.; Geohegan, A. A.; Puretzky, C. M., Rouleau , Metal-assisted hydrogen storage on Pt-decorated single-walled carbon nano horn, *Carbon.* **2012**, *50*, 4953.

[17] Vinayan, B. P.; Sethupathi, K.; Ramaprabhu, S.; Facile synthesis of triangular shaped palladium nanoparticles decorated nitrogen doped graphene and their catalytic study for renewable energy applications. *Int. J. Hydrogen Energy.* **2013**, *38*, 2240-2250, DOI: 10.1016/j.ijhydene.2012.11.091.

[18] Lee, S. M.; *et al*, Hydrogen adsorption and storage in carbon nanotubes. Synthetic Metals. **2000**, *113*, 209, DOI: 10.1016/S16310705(03)00107-5.

[19] Yildirim, T.; Ciraci, S., Titanium-decorated carbon nanotubes as a potential high-capacity hydrogen storage medium. *Phys. Rev. Lett.* **2005**, *94*, 175501, DOI: https://doi.org/10.1103/PhysRevLett.94.175501.

[20] Ye, Y.; Ahn, C. C.; Witham, C.; Fultz, B.; Liu, J.; Rinzler, A. G.; Colbert, D.; Smith, K. A.; Smalley, R. E., Hydrogen adsorption and cohesive energy of single-walled carbon nanotubes, *Appl. Phys. Lett.* **1999**, *74*, 2307, DOI: http://dx.doi.org/10.1063/ 1.123833.

[21] Liu, C.; Fan, Y. Y.; Liu, M; Conq,; H. T.; Cheng, H. M.; Dresselhaus, M. S., Hydrogen storage in single-walled carbon nanotubes at room temperature, *Science.* **1999**, *286*, 1127, DOI: 10.1126/science.

286.5442.1127.

[22] Oku, T.; Narita, I., Calculation of H_2 gas storage for boron nitride and carbon nanotubes studied from the cluster calculation, Phys. B. **2002**, *323*, 216.

[23] Dillon, A. C.; Jones, K. M.; Bekkedahl, T. A.; Kiang, C. H.; Bethune, D. S.; Heben, M. J., Storage of hydrogen in single-walled carbon nanotubes, *Natur,*. **1997**, *386*, 377-379, DOI: 10.1038/386377a0.

[24] Shahzad. Khan, M. D.; Shahid. Khan, M., Computational study of hydrogen adsorption on potassium-decorated boron nitride nanotubes, *Int. Nano. Lett.* **2011**, *1*, 103-110.

[25] Loiseau, A.; Willaime, F.; Demoncy, N.; Hug, G.; Pascard, H., Boron nitride nanotubes with reduced numbers of layers synthesized by arc discharge. *Phys. Rev. Lett.* **1996**, *76*, 4737, DOI: https:// doi.org/10.1103/PhysRevLett.76.4737.

[26] Bengu, E.; Marks, L. D., Single-Walled BN Nanostructures. *Phys. Rev. Lett.* **2001**, *86*, 2385, DOI: https://doi.org/10.1103/PhysRevLett.86.2385.

[27] Nirmala, V.; Kolandaivel, P., Structure and electronic properties of armchair boron nitride nanotubes, *J. Mol. Struct. Theochem*. **2007**, *817*, 137-145, DOI: http://dx.doi.org/10.1016/j.theochem.2007.04.033.

[28] Born, M.; Oppenheimer, J. R., Zur quatentheorie der molekeln, quantum theory of molecules, Annalen der Physik (in German). **1972**, *389*, 457-484.

[29] Hohenberg, P.; Kohn, W., Inhomogeneous electron gas. *Phys. Rev*. **1964**, *136*, B864, DOI: https://doi.org/ 10.1103/PhysRev.136.B864.

[30] Kohn, W.; Sham, L. J., Self-consistent equations including exchange and correlation effects, *Phys. Rev.* **1964**, *140*, A1133, DOI: https://doi.org/10.1103/ PhysRev.140.A1133.

[31] http://www.quantum-espresso.org/

[32] Takeda, T., The scalar relativistic approximation, *Z. Physik. B.* **1978**, *32*, 43-48, DOI: 10.1007/ BF01322185.

[33] Hestense, M. R.; Stiefel, E.; Metods of conjugate Gradients for solving linear system, *J. Research of the National Bureau of Standard.* **1952**, *49*, 6.

[34] Adsorption process of a single Na atom on (5,0) and (3,3) boron nitride nanotubes (submitted to journal).

[35] Chandrakumar, K. R. S.; Srinivasan, K.; Ghosh, S. K., Nanoscale curvature-induced hydrogen adsorption in Alkali Metal Doped Carbon Nanomaterials, J. Phys. Chem. C. 2008,112, 15670, DOI: 10.1021/jp8019446.

[36] Becke, A. D.; A multicenter numerical integration scheme for polyatomic molecules, *J. Chem. Phy.* **1998**, *88*, 2547, DOI: http://dx.doi.org/10.1063/ 1.454033.

[37] http://www.gaussian.com/.

[38] Rosi, N. L.; Eckert, J.; Eddaoudi, M.; Vodak, D. T.; Kim, J.; Keeffe, M. O.; Yaghi. O. M., Hydrogen storage in microporous metal-organic frameworks. *Science,* **2003**, *300*, 1127-1129, Rosi, N. L.; Eckert, J.; Eddaoudi, M.; Vodak, D. T.; Kim, J.; Keeffe, M. O.; Yaghi. O. M.; Hydrogen storage in microporous metal-organic frameworks. *Science,* **2003**, *300*, 1127-1129, DOI: 10.1126/science.1083440.

[39] Srepusharawoot, P.; Scheicher, R. H.; Moysés Araújo, C.; Blomqvist, A.; Pinsook, U.; Ahuja, R., *Ab initio* study of molecular hydrogen adsorption in covalent organic framework-1. *J. Phys. Chem. C.* **2009**, *113*, 8498-8504, DOI: 10.1021/jp809167b.

[40] Dillon, A. C.; Jones, K. M.; Bekkedahl, T. A.; Kiang, C. H.; Bethune, D. S.; Heben, M. J., Storage of hydrogen in single-walled carbon nanotubes, *Nature.* **1997**, *386*, 377-379, DOI: 10.1038/386377a0.

[41] Blomqvist, A.; Moysés Araújo, C.; Srepusharawoot, P.; Ahuja, R., Li decorated metal-organic framework 5: A route to achieving a suitable hydrogen storage medium, *Proc. Nat. Acad. Sci. U.S.A.* **2007**, *104*, 20173-20176, DIO: 10.1073/pnas.0708603104.

[42] Sun, Q.; Jena, P.; Wang, Q.; Marquez. M., First-principles study of hydrogen storage on. *J. Am. Chem. Soc.* **2006**, *128*, 9741-9745, DOI: 10.1021/ja058330c.

[43] Rowsell, J. L. C.; and Yaghi. O. M.; Strategies for hydrogen storage in metal organic frameworks. *Angew. Chem. Int. Ed.* **2005**, *44*, 4670-4679, DOI: 10.1002/anie.200462786.

[44] Nagare, B. J.; Habale, D.; Chacko, S.; Ghosh, S., Hydrogen Adsorption on Na/SWCNT Systems, *J. Matter. Chem.* **2012**, *22*, 22013-22021, DOI: 10.1039/

C2JM00034B.

[45] Krasnov, P. O.; Ding , F.; Singh, A. K.; Yakobson, B. I., Clustering of Sc on SWNT and reduction of hydrogen uptake: *Ab-Initio* All-electron calculations, *J. Phys. Chem. C.* **2007**, *111*, 17977-17980, DOI: 10.1021/jp077264t.

[46] http://energy.gov/eere/fuelcells/hydrogen-storage.